JOC Article
pubs.acs.org/joc

Successful Computational Modeling of Isobornyl Chloride Ion-Pair Mechanisms

Jing Kong,[†,‡] Paul v. R. Schleyer,[‡] and Henry S. Rzepa*[,§]

[†]*Key Laboratory for Green Chemical Technology of Ministry of Education, School of Chemical Engineering and Technology, Tianjin University, Tianjin 300072, China,* [‡]*Center for Computational Chemistry and Department of Chemistry, University of Georgia, Athens, Georgia 30602, and* [§]*Department of Chemistry, Imperial College London, South Kensington Campus, London SW7 2AZ, U.K.*

rzepa@imperial.ac.uk

Received May 11, 2010

Ⓦ **This paper contains enhanced objects available on the Internet at http://pubs.acs.org/joc.**

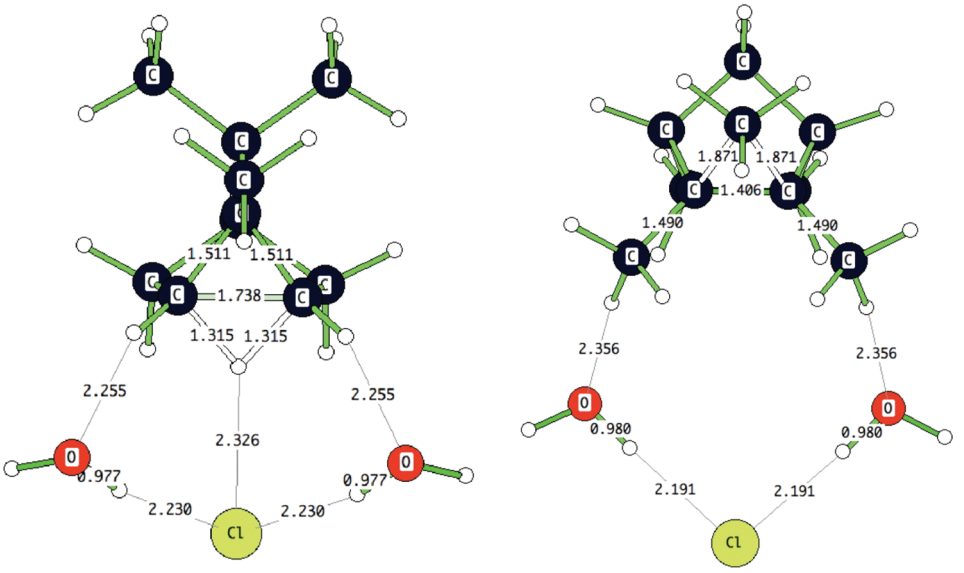

Along with the directly related Wagner−Meerwein camphene hydrochloride−isobornyl chloride rearrangement, the racemization of isobornyl chloride involves intermediate carbocation−anion ion pairs; both processes have become mechanistic icons in organic chemistry. The two known racemization pathways, involving either a hydride transfer or a methyl migration, are observed to be concurrent. However, prior quantitative computational modeling has not been able to reproduce the fine kinetic balance of these processes. We demonstrate that a density functional approach, which includes two explicit solvent molecules embedded in a continuum solvent field, coupled with full geometric optimization using smoothed solvent cavities and free energy calculation, yields results in accord with experiment. Alternative racemization routes also have been explored.

Introduction

Wagner's terpene rearrangements[1] puzzled chemists, who did not understand how they occurred. In 1922, Meerwein and van Emster[2] presented evidence that carbocation mechanisms were involved, e.g., in the reversible interconversion of camphene hydrochloride **1**′ and isobornyl chloride **2**′ (Scheme 1). Although this paper is a cornerstone of organic chemistry, unraveling the intimate nature of the intermediate

(1) (a) For an early review, see: Ruzicka, L. *Helv. Chim. Acta* **1918**, *1*, 110−133; DOI: 10.1002/hlca.1918001011 (b) Nametkin, S. S.; Briissoff, L. *Ann.* **1927**, *459*, 144-147; DOI: 10.1002/jlac.19274590109 (c) Whitmore, F. C. *J. Am. Chem. Soc.* **1932**, *54*, 3274−3283; DOI: 10.1021/ja01347a037

(2) Meerwein, H.; van Emster, K. *Chem. Ber.* **1922**, *55*, 2500−2528; DOI: 10.1002/cber.19220550829

Published on Web 07/15/2010 DOI: 10.1021/jo100920e

SCHEME 1. Ion-Pair Hydride-Shift Mechanisms for the Enantiomerization of Isobornyl Chloride (2, with Enantiomers Indicated as, e.g., 2′)[a]

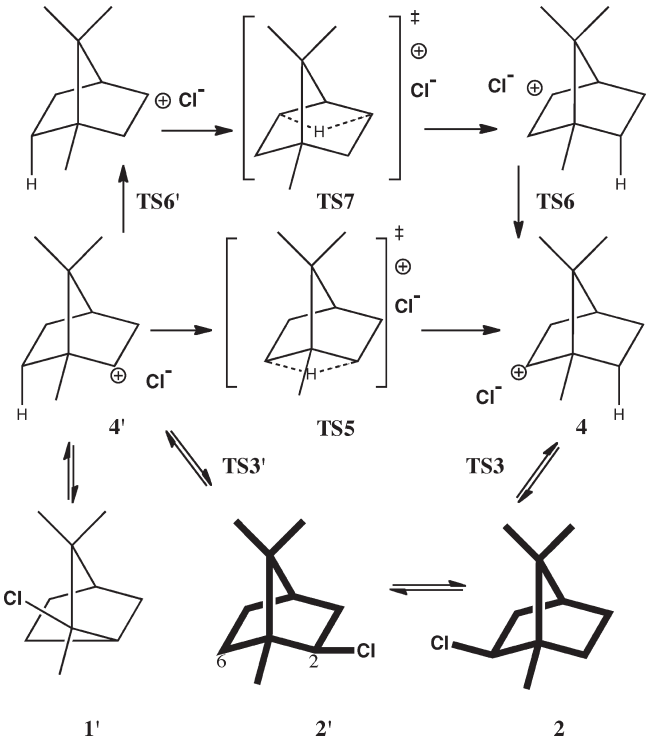

[a]Meerwein's route involved **TS5**, but an alternative via **TS7** also is possible.

camphenyl cation **4/4′** as well as all the complications and mechanistic details of this very complex system[3] has challenged chemists ever since. In 1939, Wilson and co-workers[4] recognized the nonclassical carbonium ion character of **4/4′** and studied the counterion involvement by using radioactive Cl^-. But other rearrangements besides the well-recognized Wagner−Meerwein interconversion also take place concurrently under the same reaction conditions. In 1924, Meerwein and Montfort[5] reported that the racemization of optically pure isobornyl chloride **2** or its enantiomer **2′** in *o*-cresol solution is essentially complete in ∼190 min at room temperature. No explicit Lewis acid was required to enable the reaction, although the reaction was accelerated if one is present.

As cation **4/4′** is chiral, its intervention does not suffice to explain this observation.[6] We now focus on a computational elucidation of the racemization mechanism, which illustrates how well ion-pair processes in solution can be modeled with currently available theoretical methodology. Prior computational investigations of Smith[7] and by Sorensen's group[3,8] had other objectives, as described below. Sorensen's 1975 experimental NMR study, "The Observable Thirtyfold Degenerate Camphenehydro Cation",[3] delineates the many rearrangements **4/4′** undergoes as a stable ion in super acid conditions and also is pertinent to the present investigation.

Meerwein suggested the racemization pathway **2′** to **2** illustrated in the middle of Scheme 1, which involves a 6,2-transanular hydride shift via symmetrical **TS5** following ionization of isobornyl chloride **2′** to the ion pair **4′** (shown in the classical representation). Besides the 6,2 hydride shift pathway, another competing, multistep pathway also providing a mirror point for enantiomerization can also be envisioned from **4′** to **4** via sequential 3,2- (**TS6′**), 3,5- (**TS7**), and 2,3-hydrogen shifts (**TS6**).

In 1931,[9] Houben and Pfankuch proposed an alternative 3,2-methyl migration mechanism (known then[1b] as a Nametkin rearrangement, Scheme 2), where the carbocation **4/4′** is now represented in the nonclassical form **8/8′**. Two transition states of C_s symmetry, **TS9** (*exo*) and **TS10** (*endo*), are possible. Subsequent isotopic labeling[10] and stable ion[3] studies revealed that stereoelectronically controlled *exo* Me_a migration is favored over *endo* Me_b migration and that racemization via ion pair **TS9** competed on an approximately equal basis with the pathway involving ion pair **TS5**.[10]

A fourth possible mechanism involving a symmetrical neutral intermediate **12** (tricyclene, Scheme 3), in fact, predates Meerwein's carbocation suggestion. Tricyclene was originally thought to arise from a carbene precursor **13** (the so-called Tiffeneau divalent carbon hypothesis) involving a C−H insertion reaction (**TS14**) to form **12**.[11] However, α-elimination of HCl to form such a carbene is now known not to occur under neutral or acidic conditions. This mechanism can be reformulated in a manner that avoids **13** by having a chloride anion abstract a proton from carbocation **8** with concomitant C−C bond formation to form **12** (**TS11**, Scheme 3).[12]

The most probable[13] mechanistic possibilities for enantiomerization of **2′** to **2** can be summarized as follows:

1. A hydride shift **TS5**
2. An alternative hydride shift via **TS7**
3. A shift of methyl group Me_a via **TS9** in preference to methyl group Me_b via **TS10**
4. A proton abstraction from **4/8** via **TS11** to give the mirror-symmetric tricyclene **12**.

In a recent review of this topic,[6] B3LYP/cc-pVQZ computations were presented for the cationic component only which indicated that the free energy of activation for the hydride shift **TS5** was ∼8 kcal/mol higher than that for **9** (the

(3) Haseltine, R.; Huang. E.; Ranganayakulu, K.; Sorensen, T. S. *Can. J. Chem.* **1975**, *53*, 1056−1066; DOI: 10.1139/v75-149

(4) Nevell, T. P.; de Salas, E.; Wilson, C. L. *J. Chem. Soc.* **1939**, 1188−1199; DOI: 10.1039/JR9390001188

(5) (a) Meerwein, H.; Montfort, F. *Ann.* **1923**, *435*, 207−218; DOI: 10.1002/jlac.19244350106 (b) Meerwein, H.; Wortmann, R. *Ann.* **1924**, *435*, 190−206; DOI: 10.1002/jlac.19244350105

(6) Rzepa, H. S.; Allan, C. S. M. *J. Chem. Educ.* **2010**, *87*, 221−228; DOI: 10.1021/ed800058c

(7) Smith, W. B. *J. Org. Chem.* **1999**, *64*, 60−64; DOI: 10.1021/jo980720c

(8) (a) Brunelle, P.; Sorensen, T. S.; Taeschler, C. *J. Org. Chem.* **2001**, *66*, 7294−7302; DOI: 10.1021/jo010379n

(9) (a) Houben, J.; Pfankuch, E. *Ann.* **1931**, *489*, 193−224; DOI: 10.1002/jlac.19314890112 (b) Houben, J.; Pfankuch, E. *Ann.* **1933**, *501*, 219−246. DOI 10.1002/jlac.19335010113

(10) (a) Roberts, J. D.; Yancey, J. A. *J. Am. Chem. Soc.* **1953**, *75*, 3165−3168; DOI: 10.1021/ja01109a037 (b) Vaughan, W. R.; Perry, R. *J. Am. Chem. Soc.* **1953**, *75*, 3168−3172; DOI: 10.1021/ja01109a038

(11) For early discussion of this aspect, see: Ingold, C. K. *J. Chem. Soc., Trans.* **1923**, *123*, 1706−1713; DOI: 10.1039/CT9232301706

(12) Note that camphene also undergoes acid-catalyzed racemization, which once was believed to involve tricyclene as an intermediate (ref 11), and that norbornene and nortricyclene also equilibrate readily under acidic conditions: Schleyer, P. v. R. *J. Am. Chem. Soc.* **1958**, *80*, 1700−1704; DOI: 10.1021/ja01540a047

(13) A reviewer has noted that other routes involving, e.g., collapse of the ion pair **8** into 4-(2-chloroethyl)-1,5,5-trimethylcyclopentene, followed by proton abstraction, could also effect the racemization process. An investigation of this and other aspects of the more complex fuller potential surface will be reported elsewhere.

SCHEME 2. Houben−Pfankuch Mechanism for Enantiomerization of Isobornyl Chloride 2

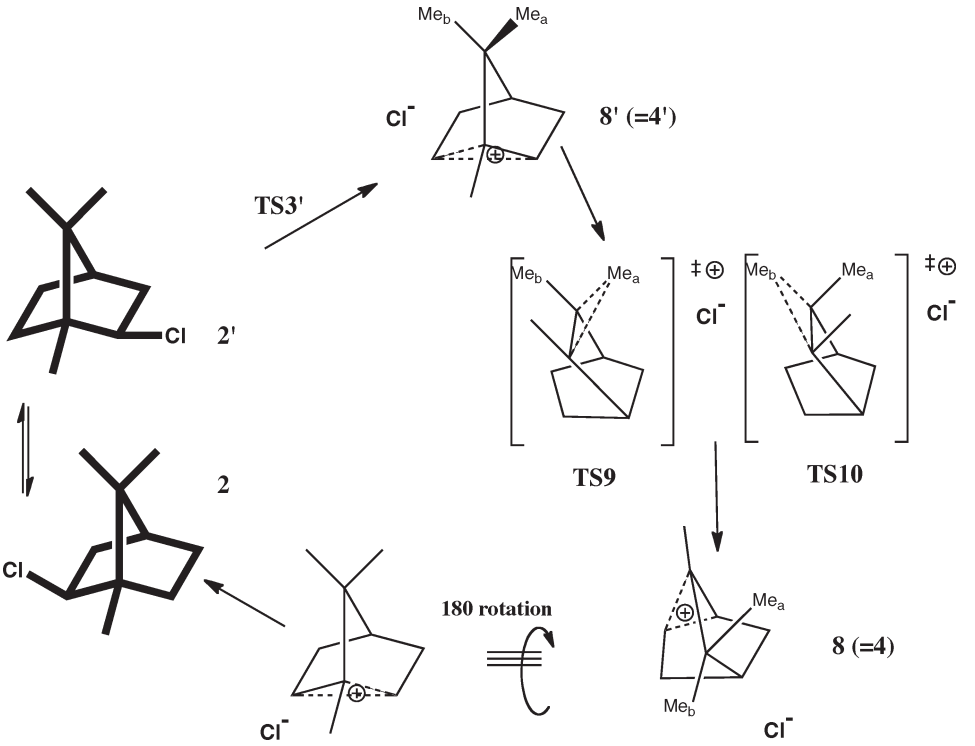

SCHEME 3. Mechanism for Enantiomerization of Isobornyl Chloride Involving Tricyclene 12

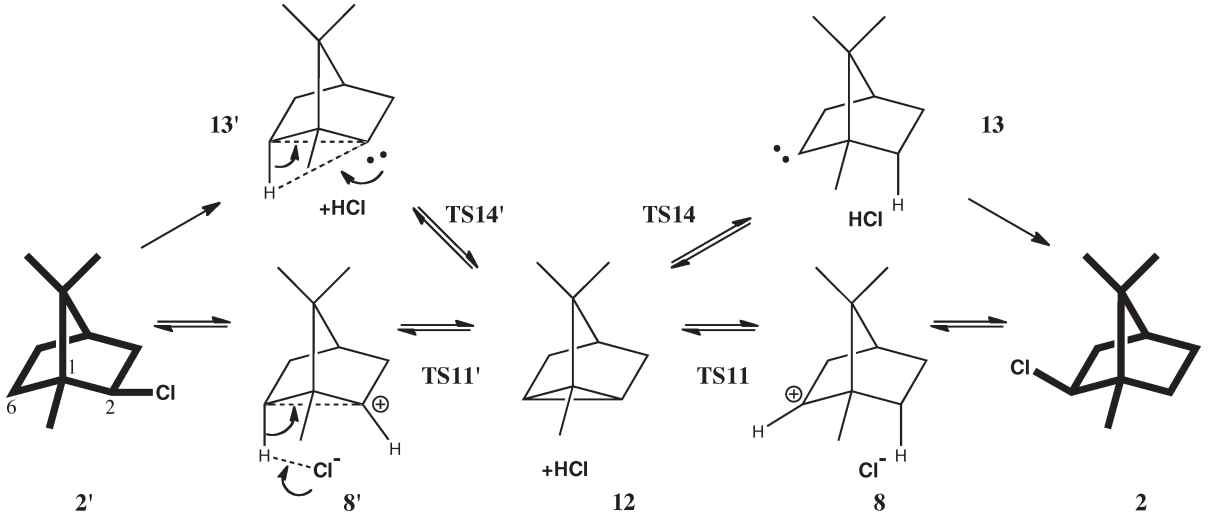

endo Me$_b$ migration **10** was significantly less favorable than **9**). The large energy difference between **5** and **9** computed at a relatively high level was thought to be incompatible with the experimentally determined concurrency of pathways. It was suggested[6] that the discrepancy might be due to a significant increase in the rate of **TS5** due to hydrogen tunneling. Differential solvation of the ion pair offers an alternative rationalization. The earlier study by Sorensen et al.[8] of the potential energy surface for skeletal rearrangements of this system showed the need for solvation energy corrections, but no direct comparison with **TS5** was made. Smith[7] explored the potential surface for interaction of **8** with chloride anion and HCl, but did not consider solvation effects. Hence, the relative energies of **5** and **8** have not been modeled previously at a consistent level of theory appropriate for explaining the enantiomerization kinetics of **2** in a polar and hydrogen bonding solvent such as cresol. We now present computations on more realistic models, which include the strong influence of the chloride counteranion as well as both bulk and explicit solvation effects. Modeling the ion-pair actually involved in solution in this manner appears to resolve the discrepancy between theory and experiment without involving tunneling.

Computational Methodologies

A key theoretical methodology in the Gaussian 09 program[14] is the introduction of smoothed solvent cavities enabling computation

TABLE 1. Relative Calculated Energies for 2−15[a]

system	water	dichloromethane	toluene	gas phase[e]
2	0.0	0.0 (1.0)[b]	0.0 (3.3)[b]	0.0 (7.9)[b,g]
	10042/to-3675[c]	10042/to-3683[c]	10042/to-3687[c]	10042/to-4916[d]
	10042/to-4883[d]	10042/to-4904[d]	10042/to-4905[d]	
TS3	15.2/116i (14.0)[d]	16.2/148i	23.2/231i	n/a
	10042/to-4877	10042/to-4893	10042/to-4891	
4/8	6.6	8.7	14.1	0.0
	10042/to-4882	10042/to-4890	10042/to-4903	
TS5	19.7/332i (21.6)[d]	21.0/319 (22.8)[d]	24.1/319i (25.7)[d]	19.2/481i
	10042/to-3676	10042/to-3678	10042/to-3682	
	10042/to-4875[d]	10042/to-4892[d]	10042/to-4894[d]	
TS6	24.5/470i (27.3)[d]	18.4/818i	20.1/409i	23.8/632i
	10042/to-4897	10042/to-4901	10042/to-4900	
	10042/to-4902			
TS7	19.7/304i	21.5/290i	24.9/273i	20.4/456i
	10042/to-4858	10042/to-4860	10042/to-4859	
TS9	18.3/329 (19.2)[d]	21.2/332i	30.2/342i	11.3/312i
	10042/to-3674	10042/to-3686	10042/to-3688	51.9/421i[f]
	10042/to-4881[d]			39.4/352i[g]
TS10	26.0/346i	31.1/345i	38.2/360i	19.4/331i
	10042/to-4866	10042/to-4862	10042/to-4864	
TS11	18.2/1017i (23.2)[d]	18.7/958i	21.1/731i	n/a
	10042/to-4867	10042/to-4868	10042/to-4869	
	10042/to-4876d			
12	5.0 10042/to-4863	6.9	7.4	7.6[g]
		10042/to-4889	10042/to-4888	
TS14	64.4/623i			62.2/620i
	10042/to-4896			
TS15	17.9/919i (23.9)[d]	18.4/818i	20.1/409i	n/a

[a]Coordinates for all stationary points, and an animation of each transition mode, are available via an interactive version of this table in the HTML version of the article. Energies (kcal/mol) are quoted as $\Delta G^{\ddagger}$, are relative to **2**, and are followed by the wavenumber of the calculated transition mode, in cm^{-1}. [b]Energy relative to water in parentheses. [c]The interactive table also includes a link to the digital identifier for an OAI-PMH compliant institutional data repository. Each link provides access to full information about each computation, including the total calculated energies via Gaussian checkpoint and logfile files, coordinates in CML form, and metadata conforming to the METS specifications. The identifier can be manually resolved as, e.g., http://dx.doi.org/10042/to-3675. [d]Single-point aug-cc-pVQZ/SCRF calculation, with no thermal corrections applied to the energy, at the optimized cc-pVTZ geometry and shown relative to **2**. [e]Cation only, excluding the $Cl^- \cdot 2H_2O$ component present in the other calculations. [f]Ion-pair, including Cl^- only. [g]Ion-pair, including $Cl^- \cdot 2H_2O$. [h]$\Delta G^{\ddagger}$ for model with one explicit water molecule, 22.1 kcal/mol; model with three explicit water molecules, 21.1 kcal/mol. [i]$\Delta G^{\ddagger}$ for model with three explicit water molecules, 20.9 kcal/mol. [j]$\Delta G^{\ddagger}$ for model with three explicit water molecules, 23.9 kcal/mol.

of continuous derivatives with respect to atomic positions and external perturbing fields.[15] This facilitates application of a polarizable continuum solvation model with rapid geometry optimization convergence and accurate Hessian (harmonic vibrational frequency) computations for stationary point characterization and zero-point energies. In addition to this continuum solvation model, it was necessary to include at least one explicit water molecule to model the original *o*-cresol solvent. After considerable testing, we selected two such solvent molecules, in part to retain the advantages of molecular symmetry. Addition of a third explicit water has only a small effect on the resulting activation free energies (Table 1, footnotes [h−j]). This assemblage was then computed at the B3LYP/cc-pVTZ level, and the putative minima and transition states were characterized. The final computed free energies include all zero-point and entropy terms, as well as free-energy terms derived from the solvent cavity, and are presented relative to **2′** or **2** (Table 1). The energies are reported for three different continuum solvents; water, dichloromethane, and toluene, representing high, medium, and low polarity media. The dielectric constant of *o*-cresol itself (6.76) lies between dichloromethane and toluene; this solvent is too large to model explicitly at the levels of theory we used.

Transition states **TS5**, **TS7**, **TS9**, and **TS10** have mirror planes of symmetry including the chloride counterion; the other stationary points (besides **12**) have no symmetry.

Results and Discussion

We first note that sensible geometries and activation barriers or relative energies are only obtained for all the various transition states or equilibrium species numbered in Schemes 1−3 if *both* continuum and discrete solvation models are combined. Direct heterolysis of R−Cl bonds (e.g., representing S_N1-type ionization reactions) cannot be modeled very meaningfully in the gas phase (the reverse recombination of two ions of opposite charge generally is barrierless) unless considerable structural reorganization takes place during the ionic dissociation.[16] The model described here does indeed give a clear-cut transition state (**TS3**) leading to the explicitly solvated nonclassical carbocation ion pair **8**.

(14) Gaussian 09, Revision A.2: Frisch, M. J.; Trucks, G. W.; Schlegel, H. B.; Scuseria, G. E.; Robb, M. A.; Cheeseman, J. R.; Scalmani, G.; Barone, V.; Mennucci, B.; Petersson, G. A.; Nakatsuji, H.; Caricato, M.; Li, X.; Hratchian, H. P.; Izmaylov, A. F.; Bloino, J.; Zheng, G.; Sonnenberg, J. L.; Hada, M.; Ehara, M.; Toyota, K.; Fukuda, R.; Hasegawa, J.; Ishida, M.; Nakajima, T.; Honda, Y.; Kitao, O.; Nakai, H.; Vreven, T.; Montgomery, J. A., Jr.; Peralta, J. E.; Ogliaro, F.; Bearpark, M.; Heyd, J. J.; Brothers, E.; Kudin, K. N.; Staroverov, V. N.; Kobayashi, R.; Normand, J.; Raghavachari, K.; Rendell, A.; Burant, J. C.; Iyengar, S. S.; Tomasi, J.; Cossi, M.; Rega, N.; Millam, N. J.; Klene, M.; Knox, J. E.; Cross, J. B.; Bakken, V.; Adamo, C.; Jaramillo, J.; Gomperts, R.; Stratmann, R. E.; Yazyev, O.; Austin, A. J.; Cammi, R.; Pomelli, C.; Ochterski, J. W.; Martin, R. L.; Morokuma, K.; Zakrzewski, V. G.; Voth, G. A.; Salvador, P.; Dannenberg, J. J.; Dapprich, S.; Daniels, A. D.; Farkas, Ö.; Foresman, J. B.; Ortiz, J. V.; Cioslowski, J.; Fox, D. J. Gaussian, Inc., Wallingford, CT, 2009.

(15) (a) Scalmani, G.; Frisch, M. J. *J. Chem. Phys.* **2010**, *132*, 114110−114115; DOI: 10.1063/1.3359469 (b) York D. M.; Karplus, M. *J. Phys. Chem. A* **1999**, *103*, 11060−11079; DOI: 10.1021/jp992097l

(16) Rzepa, H. S. URL: http://www.ch.ic.ac.uk/rzepa/blog/?p=1135. Accessed: 2010-04-26. (Archived by WebCite at http://www.webcitation.org/5pHRDIOSD.)

The balance between the energy of the solvated C−Cl heterolysis and the strain-relieving skeletal rearrangement to the nonclassical geometry results in a free energy barrier for **TS3** (15.2 kcal/mol in water); this barrier increases, as expected, in less polar continuum media, rising to 23.2 kcal/mol in toluene (with two waters as the explicit solvation throughout). The product of this ionization **4** is lower than **TS3**, implying a clear barrier for reverse recombination.

However, the rate-limiting step for racemization involves the higher barriers associated with later stages involving C_s-symmetric transition states, such as **TS5** or **TS9** in particular. Increasing the polarity of the continuum decreases the energy of **TS9** to a greater extent than that of **TS5**. While **TS5** has a distinctly lower energy than **TS9** in simulated toluene, both are predicted to be equally stable in solvents like dichloromethane. In contrast, a water-based continuum favors **TS9** modestly. Although the methyl migration alternative **TS9** would be entirely inhibited in nonpolar solvents, the free energy barrier for **TS5** or **TS9** (~18−21 kcal/mol in the water to dichloromethane solvent range) is consistent not only with Meerwein's report that racemization is "essentially complete in ~190 min"[5] but also with the labeling studies establishing that the rates of both racemization processes are competitive.[10] The quite different dipole moments of the two transition states (12.8D for **TS5**, 21.3D for **TS9**) explain why the relative energies of the two pathways are influenced so strongly by solvent polarity. As is apparent from the structures shown below, the separation of the cationic and anionic moieties of **TS5** (Figure 1) is much smaller than that of **TS9** (Figure 2). This accounts for the large difference in their dipole moment as well as their energy responses to changes in continuum solvation. Like the gas-phase cation model and Sorensen's experimental finding,[3] **TS10** (for 3,2 *endo* methyl migration) is disfavored over **TS9** (3,2 *exo* methyl migration), because of a significant stereoelectronic effect.[6]

The relative energies of the isolated cations by themselves (without the anionic counterions, explicit water, or a continuum medium) predict different behavior[6] and favor **TS9** over **TS5** by nearly 8 kcal/mol! Without either continuum or explicit solvation, it was still possible to compute **TS9** as a (gas phase) ion pair with Cl^- present, but the free energy barrier was unfeasibly high (51.9 kcal/mol). Including just the explicit solvent in the form of two water molecules reduced the barrier to 39.4 kcal/mol. The alternative hydride transfer **TS5** could not be located as a transition state using either of these reduced models or, indeed, with just the continuum model and no explicit water. Instead, the chloride anion now abstracts the migrating hydrogen to form a weak hydrogen-bonded cyclopropane-like complex[17] **12** between HCl and tricyclene. Only when both explicit and continuum solvents are included is the **TS5** located (Figure 1). The geometry is characterized by hydrogen-bonding interactions involving the chloride counteranion and the transferring hydrogen atom as well as with the two discrete water molecules. The two oxygens of the latter also interact with covalently bound hydrogens on carbons 1 and 6. The 331i cm^{-1} imaginary frequency for the transition mode of **TS5** is remarkably low for such a migration of a light hydrogen atom. The competing methyl shift **TS9** has a slightly lower

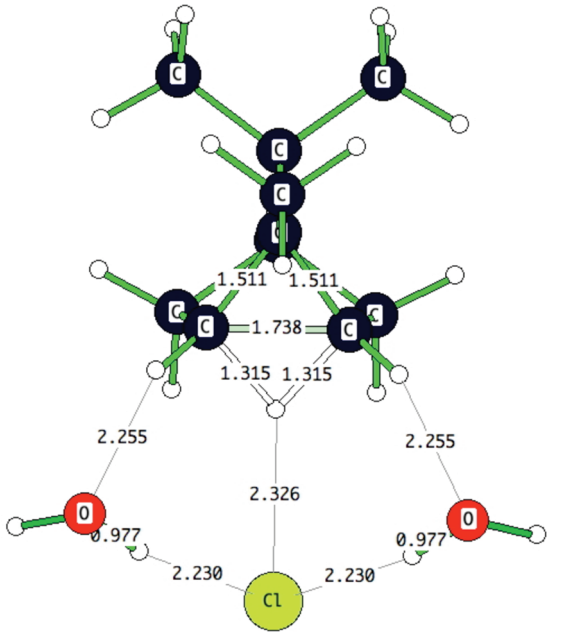

FIGURE 1. Transition state **TS5** (C_s symmetry) for 6,2 hydride migration, computed as an explicitly solvated ion-pair model (B3LYP/cc-pVTZ/SCRF). Bond lengths in Å. Dipole moment (in water as continuum solvent) 12.8 D.

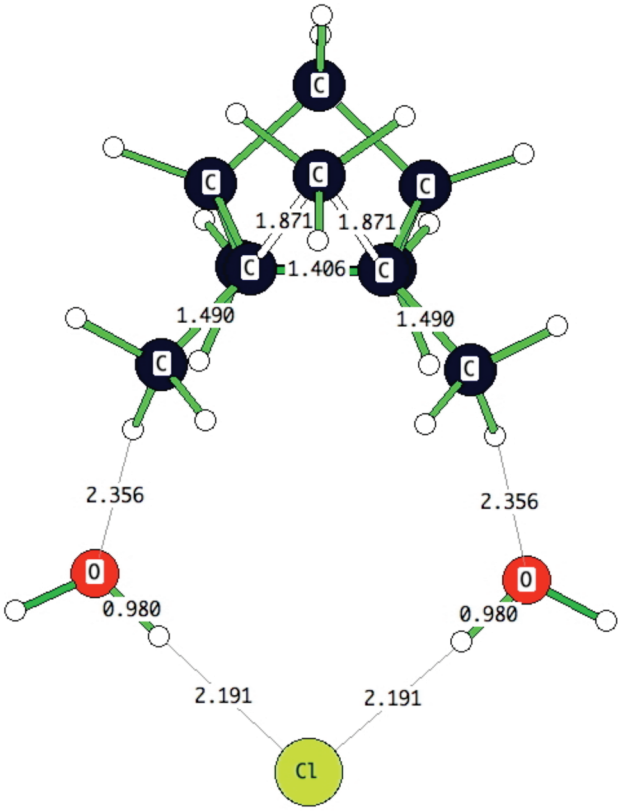

FIGURE 2. TS9 (C_s symmetry) for 3,2-*exo* methyl migration, computed as an ion-pair model. Bond lengths in Å. Dipole moment (in water as continuum solvent) 21.3 D.

barrier (18.3 vs 19.7 kcal/mol for **TS5** in water simulation). The explicitly water-solvated chloride counteranion in **TS9** (Figure 2) fits into a pocket on the opposite side of the

(17) Joris, L.; Schleyer, P. v. R.; Gleiter, R. *J. Am. Chem. Soc.* **1968**, *90*, 327−336; DOI: 10.1021/ja01004a022

SCHEME 4. Competing Proton Abstraction and Hydrogen Migration Pathways for Isomerization of 4′ to 4

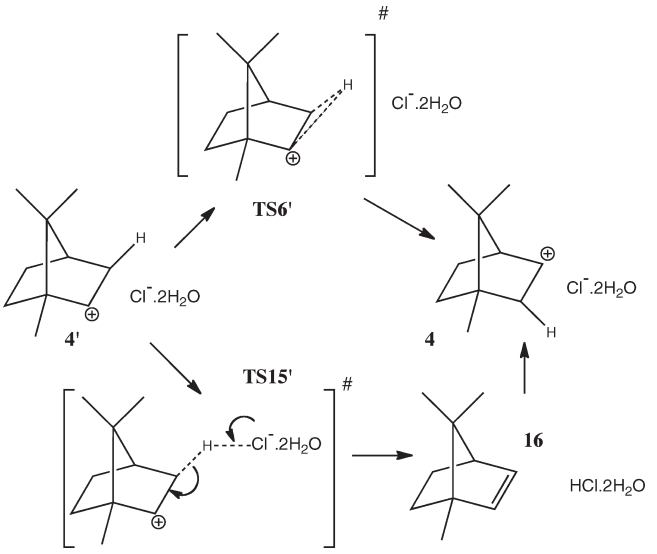

migrating methyl group, where the two relatively strong methyl C−H···O interactions shown help stabilize the arrangement. As noted above, the computed dipole moment of the more compact **TS5** (12.8 D, Figure 1) is considerably less than that of the more extended **TS9** (21.3 D, Figure 2), consistent with the energetic effects of changing the continuum (Table 1).

The third mechanistic alternative for racemization is a variation on **TS5** via the sequence (a) 3,2 hydride shift (**TS6′**), (b) 3,5 hydride shift (**TS7**), (c) 2,3 hydride shift (**TS6**, Scheme 1). During the course of locating **TS6/6′**, we noticed the incursion of a competing stepwise pathway (Scheme 4) involving proton abstraction by chloride anion to form bornene **16** via **TS15** (a reprotonation, as shown in Scheme 4, would, however, be unlikely if, e.g., the solvent were to sequester the HCl formed). With water as continuum solvent, both pathways are found to exist, but for dichloromethane and toluene, only the stepwise pathway is identified. While the synchronous **TS6** is ~5 kcal/mol higher than **TS5**, the stepwise **TS15** appears (at this level of theory, but see the caveat about using a better basis set level below) to offer a more accessible bypass for access to **TS7** and hence racemization (Table 1).

Like **TS15**, **TS11** is another base-induced (chloride anion) proton transfer that addresses the alternative mechanism described in Scheme 3. This transition state has not, to our knowledge, been studied previously. The product now is tricyclene **12**, not a product observed to form in the cresol reaction.[5] In agreement with this observation, **12** is calculated to be higher in free energy than **2**, so much that any equilibrium concentration of **12** would be vanishingly small. At this point, we note that the barriers for proton abstraction (**TS11**, **TS15**) were relatively lower in energy compared to the migration reactions. A rather better diffuse basis set description of the chloride anion (aug-cc-pVQZ) used in a single-point calculation of the energy (Table 1) reverses this ordering. Using this last model, our best estimate of the ordering of the various transition states involved in the racemization of isobornyl chloride is **TS3** < **TS9** ~ **TS5** < **TS11** ~ **TS15** < **TS10** ≪ **TS14** (in water as continuum/explicit solvent). The energy of **TS14**, the barrier for the classic Tiffeneau mechanism involving generation and insertion of carbene **13** into the β C−H bond, is implausibly high.

Conclusions

The clear conclusion emerges that the fine balance observed experimentally between the two competing isobornyl chloride racemization pathways represented by **TS5** and **TS9** only is reproduced by sophisticated computational modeling. As the energies of the corresponding carbocation transition structures differ considerably, it is necessary to include the Cl^- counterion, explicit solvation by two explicit water molecules, and further solvation modeled with a continuum field in order to achieve good agreement with the experimental findings. The dipole moments of the best competing transition structure models, **TS5** and **TS9**, differ considerably. This accounts for the difference in response of their energies to changes in their environment.

The availability of the new computational methodology employed here (smoothed solvent cavities with continuous energy derivatives)[14,15] facilitates the routine application of theory to investigate potential energy surfaces where variation in polarity may be substantial and to characterize transition states on the basis of their free energies. In the present case, finding the optimal position of the intimate counterion (a solvated chloride anion) involved only a small number of possibilities, which was explored easily for the systems described here. But much more complex cases are likely. Consequently, PES explorations raise the stochastic issue of ensuring completeness. Not only are there many possible minima, but even more mechanistic pathways between them. Nevertheless, we note that reports of such explorations involving close or intimate ion-pair species already are appearing.[18]

Acknowledgment. We dedicate this paper, with warmth, to Ted S. Sorensen in recognition of his 75th birthday. We thank the China Scholarship Council (CSC) for a graduate study grant to J.K. (File No. 2008625104). The work was supported in Georgia by NSF Grant No. CHE-0716718. We thank Dieter Lenoir for his interest and for pointing out Meerwein's remarkably prescient description, "a precursor, which rearranges easily, forms initially during the addition of HCl to camphene," which can be regarded as a "pre-theory" of ion pairing.

(18) (a) Kong, J.; Roy, D.; Lenoir, D.; Zhang, X. W.; Zou, J. J.; Schleyer, P. v. R. *Org. Lett.* **2009**, *11*, 4684−4687; DOI: 10.1021/ol901984x (b) Smith, A.; Rzepa, H. S.; White, A.; Billen, D.; Hii, K. K. *J. Org. Chem.* **2010**, *75*, 3085−3096; DOI: 10.1021/jo1002906 (c) B. Galabov, B.; Koleva, G.; Schleyer, P. v. R.; Schaefer, H. F., III. *J. Org. Chem.* **2010**, *75*, 2813−2819; DOI: 10.1021/jo902730g (d) Jin, P.; Li, F.; Riley, K.; Lenoir, D.; Schleyer, P. v. R; Chen, Z. *J. Org. Chem.* **2010**, *75*, 3761−3765; DOI: 10.1021/jo100535n